Journal of Functional Foods 83 (2021) 104573

Contents lists available at ScienceDirect

Journal of Functional Foods

journal homepage: www.elsevier.com/locate/jff

Nanoparticles derived from porcine bone soup attenuate oxidative stress-induced intestinal barrier injury in Caco-2 cell monolayer model

Guanzhen Gao [a], Jianwu Zhou [a], Yongyang Jin [a], Huiqin Wang [a,*], Yanan Ding [a], Jingru Zhou [a], Lijing Ke [a], Pingfan Rao [a], Pik Han Chong [a], Qiang Wang [b], Longxin Zhang [c]

[a] Food Nutrition Science Centre, School of Food Science and Biotechnology, Zhejiang Gongshang University, Hangzhou, Zhejiang, China
[b] Institute of Food Science and Technology, Chinese Academy of Agricultural Sciences, Beijing, China
[c] Fujian Provincial Maternity and Children Hospital, affiliated hospital of Fujian Medical University

ARTICLE INFO

Keywords:
Bone soup
Nanoparticles
Oxidative stress
Intestinal barrier injury
Caco-2 cell monolayer
AAPH

ABSTRACT

Safety concerns arose on the interaction between nanoparticles in food and intestinal tract. Food components could spontaneously assemble into a large number of nanoparticles during food processing. These nanoparticles may possess physiological effects differed from those of constituent components, are worth paying attention to, but are barely investigated yet, especially on their interaction with intestinal tract. Porcine bone soup is rich in nanoparticles, which can directly interact with oral macrophages disclosed by our previous study. In this study, the effects of bone soup nanoparticles on intestinal barrier function were subsequently evaluated on Caco-2 cell monolayers. The results revealed the nanoparticles did not develop but restore intestinal barrier dysfunction compared with engineered nanoparticles, indicated by barrier integrity, sodium fluorescein permeability, tight junctions and adherent junctions related proteins. These results showed the potential of bone soup nanoparticles on improving intestinal disorders, which resonated with traditional knowledge on the efficacies of bone soup.

1. Introduction

Nanoparticles (NPs) are able to enter, translocate within, and damage living organisms. This ability results from their unique physicochemical properties such as small size and charged surface, which allow them to penetrate physiological barriers and produce adverse physiological effects (Buzea, Pacheco, & Robbie, 2007). Due to the substantial increasing use of the engineered nanomaterials (ENMS) in food and agricultural products, more safety concerns arose on the interaction between ENMs and intestinal tract (McClements & Xiao, 2017). For instance, Ag NPs can disrupt intestinal cells' permeability, decrease cell viability and induce both the inflammation and oxidative stress (Martirosyan, Polet, Bazes, Sergent, & Schneider, 2012). TiO_2 NPs produced statistically significant injury on the barrier's integrity and increased permeability (Brun et al., 2014; García-Rodríguez, Vila, Cortés, Hernández, & Marcos, 2018), and these adverse effects were found *in vivo* (Ruiz et al., 2017). Disruption in cell membrane integrity and increased cell leakage were also seen in the Caco-2 cells treated with SiO_2 and ZnO NPs (Mortensen et al., 2020; Vita, Royse, & Pullen, 2019).

Besides ENMs, abundant amounts of nanoparticles, which were spontaneously assembled by food endogenous components during food processing, widely exist in daily foods (Cao et al., 2017; Cong et al., 2019; Jiang, Shi, Li, Xiong, & Sun, 2019; Ke et al., 2017; Li, Jiang, Wang, Cong, & Tan, 2018; Lin et al., 2017; Wang et al., 2019). In freshwater clam (*Corbicula fluminea* Muller) soup, a large amount of nanoparticles with sizes ranged from 40 nm to 149 nm formed during boiling (Gao et al., 2021; Ke, Zhou, Lu, Gao, & Rao, 2011). The colloidal particles with a mean size of 50–100 nm were produced by tea brewing of green tea (Lin et al., 2017). The nanoparticles were also found in the prepared traditional Chinese medicine decoctions, e.g. the Ma-Xing-Shi-Gan decoction which contains rich amount of nanoparticles with sizes ranged from 65 nm to 138 nm (Zhou et al., 2014). In this regard, human digestive tract has been exposed to numerous nanometer-sized particles from daily foods. These nanoparticles may possess physiological effects

Abbreviations: NPs, Nanoparticles; ENMS, Engineered nanomaterials; GI, Gastrointestinal; TEER, Transepithelial/transendothelial electrical resistance; TJs, Tight junctions; AJs, Adherent junctions; AAPH, 1,1-Diphenyl-2-picrylhydrazyl radical 2,2-Diphenyl-1-(2,4,6-trinitrophenyl) hydrazyl; FL, Sodium fluorescein; CI, Cell Index; SEC-DLS, Size-exclusion chromatography coupled with a dynamic light scattering detector; TEM, Transmission electron microscope; IBD, Inflammatory bowel disease; UC, Ulcerative colitis; IBS, Irritable bowel syndrome.

* Corresponding author at: 1st Lab Building, Food Nutrition Center, Zhejiang Gongshang University, Hangzhou, China.
E-mail address: huiqinwang@zjgsu.edu.cn (H. Wang).

https://doi.org/10.1016/j.jff.2021.104573
Received 4 February 2021; Received in revised form 30 May 2021; Accepted 2 June 2021
Available online 10 June 2021

that differ from those of constituent components, and they are worth paying attention to, although they have received little attention and investigation thus far, particularly in terms of their interaction with the intestinal tract.

The intestinal barrier in the gastrointestinal (GI) tract plays a vital role in protecting the internal environment from ingested particles at micro and nano scales (Iacob & Iacob, 2019; Salvo-Romero, Alonso-Cotoner, Pardo-Camacho, Casado-Bedmar, & Vicario, 2015; Sinnecker, Krause, Koelling, Lautenschläger, & Frey, 2014). The intestinal epithelial barrier function, which can be assessed by transepithelial/transendothelial electrical resistance (TEER), paracellular permeability, localization of tight junctions (TJs) and adherent junctions (AJs), is widely adopted for evaluating the cytotoxic effects of this interaction (Bergin & Witzmann, 2013; Lefebvre, Venema, Gombau, & L. G. V., Raju, J., Bondy, G. S., Bouwmeester, H., Singh, R. P., Amy, J., Collnot, E., Mehta, R., Stone, V., Raju, J., Bondy, G. S., Bouwmeester, H., Singh, R. P., & Clippinger, A. J. , 2015; Vila, García-Rodríguez, Cortés, Marcos, & Hernández, 2018). Besides, an impedance-based xCELLigence Real-Time Cell Analyzer (RTCA) system also has been applied to monitor the barrier function due to its real-time, continuous, and dynamic monitoring (Sun et al., 2012).

As a traditional nourishing food worldwide, bone soup is widely used as a folk remedy for preventing and treating immune malfunction, inflammatory bowel disease and insulin insensitivity (Mizokami et al., 2016; Morell & Daniel, 2014; Siebecker, 2005). Well prepared porcine bone soups are rich in nanoparticles. The number of NPs in every millilitre of porcine bone soup even reaches billion. These NPs can directly interact with oral macrophages and remained intact in a few hours after engulfment by oral macrophages, producing significant effects on preventing cells from peroxyl radical induced membrane hyperpolarization, mitochondrial malfunction and phagocytosis suppression (Ke et al., 2017). Whether these NPs are capable to interact with intestinal cells are subsequently investigated in this study. In this study, nanoparticles isolated from porcine bone soup were subjected to investigate their interaction with the intestinal barrier on Caco-2 cell monolayer, examining their cytotoxicity, cytoprotection from oxidative stress-induced intestinal barrier injury by 1,1-Diphenyl-2-picrylhydrazyl radical 2,2-Diphenyl-1-(2,4,6-trinitrophenyl) hydrazyl (AAPH) in Caco-2 cell monolayer.

2. Materials and methods

2.1. Preparation of nanoparticles derived from porcine bone soup

The fresh porcine bones from the Landrace pigs (*Sus scrofa*) were obtained from the fresh local market. The bone soup was prepared according to our previous report (Ke et al., 2017; Wang et al., 2019). Briefly, after the removal of the blood residues, the bone was cut into small pieces and cooked with deionized water for 3 h in a boiling water bath. The porcine bone nanoparticles were isolated with a pre-equilibrated size-exclusive chromatographic column (Sephacryl S-1000 SF from GE Health, USA, 1.0 × 100 cm, 0.02 M phosphate buffer, pH 7.4). The fractions with strong light scattering were collected and marked as bone soup NPs. The hydrodynamic diameter, ζ-potential, and PDI of bone soup NPs were characterized using Zetasizer Nano-ZS (Malvern Instruments Ltd., Malvern, UK) at 25 °C. The particle numbers of bone soup NPs were detected by Nanosight NS300 (Malvern Instruments Ltd., Malvern, UK) based on Nanoparticle Tracking Analysis (NTA) technology at 25 °C. The bone soup NPs were then subjected to the 300-mesh copper grid, stained with 5% uranyl acetate, and observed on a transmission electron microscope (TEM, Joel JEM-1230, Tokyo, Japan) at 80 kV. The contents of protein, lipid and carbohydrate were determined by using Bicinchoninic acid (BCA) assay, GPO-PAP assay and anthrone-sulfuric acid assay, separately. Gel electrophoresis analysis of bone soup NPs were performed with SDS-PAGE.

2.2. Cell culture

Caco-2 cells were provided by Stem Cell Bank, Chinese Academy of Sciences (Shanghai, China). The cells were cultured in MEM medium (Gibco, Life Technologies Corporation, Grand Island, NY, USA) containing 10% FBS (BOVOGEN, Victoria, Australia), 100 U/mL penicillin, and 100 U/mL streptomycins (Gibco, Life Technologies Corporation, Grand Island, NY, USA). The cells were passaged by partial digestion with 0.25% trypsin-EDTA (Gibco, Life Technologies Corporation, Grand Island, NY, USA) in a humidified 37 °C, 5% CO_2 incubator. Cells from passages 20–40 were used for all of the experiments.

2.3. Measurement of cytotoxicity of bone soup NPs on Caco-2 cell

According to previous work (Kowapradit et al., 2010), the cytotoxicity of bone soup NPs on Caco-2 cells was tested by MTT assay. Briefly, Caco-2 cells (1×10^4 cells/well) were seeded into 96-well plates and placed at 37 °C in a 5% CO_2 incubator overnight. The control, tested and blank group were then set with five duplicate wells for each group. 200 μL of sample was added at the concentration of 3.00, 1.50, 0.75 and 0.38×10^9 particles/mL or basic culture medium to each well. After 24 h, the supernatant was removed and washed twice with PBS, piped MTT solution (5 mg/mL) 50 μL/well to the whole plate and then placed at 37 °C for 4 h. The MTT solution was carefully removed, washed once with PBS, and 150 μL/well DMSO was added with continuous shaking until crystallization was fully dissolved. The absorbance was read at 570 nm (OD) and the cell viability was calculated according to the following formula:

$$\text{Cell viability}(\%) = \frac{(\text{OD}_{\text{sample}} - \text{OD}_{\text{blank}})}{(\text{OD}_{\text{control}} - \text{OD}_{\text{blank}})} \times 100\% \quad (1)$$

2.4. Influence of NPs isolated from porcine bone soup on Caco-2 intestinal monolayer cells paracellular permeability disruption induced by AAPH

Caco-2 cells were seeded into the 0.4-μm permeable filters (1.2 mm, 24 well, costar 3470, Corning, NY, USA) at an average density of 1×10^5 cells/well, placed at 37 °C in a 5% CO_2 incubator and the culture medium was changed on an alternative day until 21 days to form cell monolayers. The wells whose TEER value up to 600 Ω·cm^2 were used for experiments. The Caco-2 cell monolayers were incubated in the cell culture medium control or treated with AAPH (20 mM) plus 3.00, 2.25, 1.50×10^9 particles/mL NPs isolated from porcine bone soup for 6 h.

The transepithelial electrical resistance (TEER) of Caco-2 intestinal monolayer cells was measured by Millicell ERS 2 (Millipore, Bedford, MA, USA) based on the manufacturer's instructions. Both the apical and basolateral sides of the epithelium were washed three times with HBSS before the measurements. TEER was recorded and calculated as Ω × cm^2. The background resistance caused by the membrane insert was corrected. The immediate time (0 h) and the interaction time (6 h) of TEER value were measured to calculate the changes of TEER according to the following formula:

$$\text{TEER}\% = \frac{\text{TEER}_{6h}}{\text{TEER}_{0h}} \times 100\% \quad (2)$$

Sodium fluorescein (FL) was applied to determine paracellular permeability as described previously (Wang et al., 2012) with a final concentration of 2 mg/L in the basal well. After 6 h treatment, 100 μL culture medium was taken out from each apical well and measured the fluorescence value with excitation at 485 nm and emission at 525 nm in a FlexStation® 3 Multi-Mode Microplate Reader (Molecular Devices, Sunnyvale, CA). According to the standard curve of FL, the concentration of FL was calculated and the permeability rate of FL was obtained using the following formula:

$$\text{FL permeability rate}\left(\%\ /\text{hr}/\text{cm}^2\right) = \frac{\text{FL}_{\text{basolateral}} \div \text{FL}_{\text{apical}}}{\text{T}_{(\text{interaction time})} \times \text{A}_{(\text{surface area})}} \times 100\% \quad (3)$$

2.5. Real-time monitoring of Cell Index response profiles of Caco-2 cells

The xCELLigence Real-Time Cell Analyzer (RTCA) system is a non-invasive, label-free, impedance-based biosensor system, which has been applied for assessing epithelial barrier function *in vitro* (Sun et al., 2012). The detailed procedures for the xCELLigence RTCA system (xCELLigence RTCA SP, ACEA Bioscience Inc., San Diego, CA, USA) have been described previously (Sun et al., 2012). Briefly, 50 μL MEM basic media were piped into 16-well E-plate to obtain background reading, followed by the addition of 150 μL Caco-2 cell suspensions (1×10^5 cells/well). The E-plant was incubated at room temperature for 30 min before being placed onto the reader in the incubator (37 °C, 5% CO_2) for real-time measurement of cell response. The culture medium was changed every 24 h. Experiments were performed 21 days post-confluence. After the E-plant was fully covered by cells in a stable state, the system normal Cell Index (CI) value was defined as 1. The culture medium was then removed, AAPH (20 mM) and samples were successively added to record continuously record the data for 6 h, the impedance was denoted as CI.

2.6. Investigation of bone soup NPs on Caco-2 cell monolayer by immunofluorescence microscopy

Caco-2 cells were seeded into a 35-mm glass cell culture dish and incubated at 37° C in a 5% CO_2 incubator until forming monolayer. The cell monolayers were treated with the cell culture medium, AAPH (20 mM), NPs isolated from porcine bone soup (3.00×10^9 particles/mL), or AAPH (20 mM) plus NPs isolated from porcine bone soup (3.00×10^9 particles/mL) for 6 h. The solutions were then carefully removed. The cells were fixed with Immunol Staining Fix Solution for 10 min at room temperature, washed twice with Immunol Staining Wash Buffer for 5 min each, blocked with QuickBlock™ Blocking Buffer at room temperature for 10 min. Samples were incubated with anti ZO-1 Alexa 594-conjugated antibody (1:100, 339194, Invitrogen, NY, USA), E-cadherin Alexa 488-conjugated antibody (1:100, 53–3249-82, Invitrogen, NY, USA), and Rhodamine Phalloidin (1:40, R415, Invitrogen, NY, USA) overnight at 4 °C, then washed with washing buffer. Before observing, samples were stained with Hoechst 33,342 and then washed. The excitation wavelength/emission wavelength for F-actin, ZO-1, Cadherin, and Hoechst33342 are 540/564 nm, 590/617 nm, 498/520 nm, and 346/460 nm, separately.

2.7. Statistical analysis

Data analyses were performed with GraphPad Prism 5.0 (GraphPad Software, Inc., San Diego, CA). All experimental data were representative of three independent experiments and expressed as the mean values ± S.D ($n = 3$ or 5) for each measurement. Student's *t*-test was applied to examine the data significant levels. A P value < 0.05 indicate significant difference.

3. Results

The preparation of nanoparticles derived from porcine bone soup were described previously (Ke et al., 2017; Wang et al., 2019). The porcine bone soup was isolated by size-exclusion chromatography coupled with a dynamic light scattering detector (SEC-DLS), as shown in Fig. 1A. The hydrodynamic diameter, ζ-potential, and PDI of bone soup

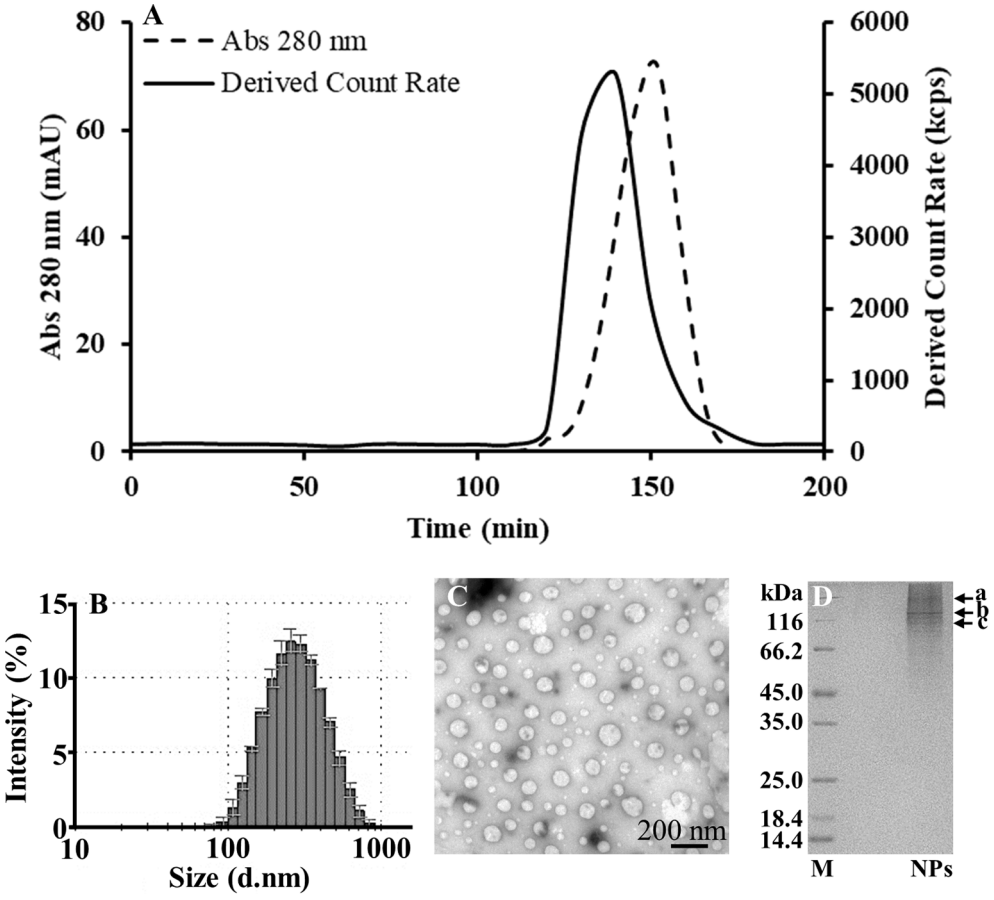

Fig. 1. Isolation and characterization of porcine bone soup NPs. (A) Isolation of porcine bone soup NPs with SEC. Bone soups were fractioned by a Sephacryl S-1000 SF column (1.0 × 50 cm) equilibrated with 0.05 M phosphate buffer (pH 7.0). The column was eluted with the same buffer at a flow rate of 0.5 mL/min at 40 °C with UV and Zetasizer Nano-ZS (Malvern, UK). SEC chromatogram of bone soup was exhibited as the Derived Count Rate (solid line) and UV absorbance at 280 nm (dash line); (B) Diameter distribution profiles by the intensity of bone soup NPs. (C) TEM micrographs of porcine bone soup NPs, magnification × 20,000. (D) Gel electrophoresis analysis of porcine bone soup NPs. M: Marker; NPs: porcine bone soup NPs; a: collagen β-chain, b: collagen α1 chain, c: collagen α2 chain.

NPs were 224 ± 4.8 nm, −14.6 ± 3.4 mV, and 0.2 ± 0.01, separately (Table 1). The nanoparticle number was counted as 8.46 ± 0.9 × 10^9 particles/mL by Nanoparticle Tracking Analysis (NTA). The morphology of bone soup NPs was observed by transmission electron microscope (TEM), exhibiting an appearance of spheres with uniform size (Fig. 1C). Moreover, as shown in Table 2, the lipids, proteins and carbohydrates content of bone soup NPs, were 45.26%, 19.19% and 10.75%, separately. Gel electrophoresis analysis of constituent proteins revealed that bone soup NPs included α1, α2 and β-chain of collagen (Fig. 1D). These properties of bone soup NPs were consistent with the previous report (Wang et al., 2019).

The cytotoxicity effects of NPs from porcine bone soup on Caco-2 cells were evaluated by MTT assay, as shown in Fig. 2. The cell viability reached over 80%, suggesting that NPs at tested concentration were non-cytotoxic on Caco-2 cells. According to the results, three concentrations of 3.00, 2.25 and 1.50 × 10^9 particles/mL were chosen for further investigations.

Treatment with AAPH decreased the TEER of Caco-2 monolayers to 17.4% ($p < 0.01$) after 6 h (Fig. 3A) compared with the TEER value of control, indicating that the oxidative stress damage caused by AAPH impaired the barrier function of Caco-2 cells. Meanwhile, co-treatment with AAPH and NPs in 6 h also caused significant change of TEER value. When comparing with the AAPH group, NPs at 3.00, 2.25, and 1.50 × 10^9 particles/mL rose the TEER values to 62.5%, 23.6%, and 35.6%, separately, indicating that the NPs notably restored the barrier function of Caco-2 cells in a dose-independent manner (Fig. 3A). Among the concentrations, 3.00 × 10^9 particles/mL of the NPs showed the best efficacy on protecting the barrier function from AAPH-induced oxidative damage.

A reduction in the barrier's integrity and stability of Caco-2 cell monolayers usually causes an increase of permeability (Peng, He, Chen, Holzman, & Lin, 2007). As a paracellular marker, FL is widely used to measure the permeability of cells monolayer (Wang et al., 2012). As shown in Fig. 3B, in the presence of AAPH, the FL permeability of Caco-2 cell monolayer increased dramatically from 0.7% to 12.7% hr/cm^2 ($P < 0.01$), indicating an increase in intercellular permeability resulted from the oxidative stress damage. Meanwhile, incubation of Caco-2 cells together with AAPH and NPs mostly or partially reduced intercellular permeability in a dose-independent manner. The NPs at both 3.0 and 1.50 × 10^9 particles/mL exhibited significant influences on recovering intercellular permeability. The results suggest that incubation together with the NPs can protect the barrier function and recover the intercellular barrier permeability on APPH-treated Caco-2 cell monolayer.

The xCELLigence Real-Time Cell Analyzer (RTCA) system has been applied to access epithelial cell barrier function using electrical impedance (shown as 'Cell Index (CI)') (Sun et al., 2012). The change of impedance reflect the alterations in barrier function and permeability (Atienza et al., 2006). When compared with the control group, the normalized CI value of Caco-2 cells was significantly decreased at the presence of AAPH, a peroxyl free radicals' inducer (Fig. 4), indicating that AAPH-induced oxidation stress impaired the cell barrier function and led to an increase in cell permeability. The normalized CI value of the AAPH group decreased to 0.9 in the first 20 min, followed by a gradually increased to 0.95 at 90 min and eventually remained constant. It indicated that AAPH induced oxidative stress in Caco-2 cells, which occurred mainly in the first 90 min.

Table 1
The properties of bone soup NPs.

Sample	PDI	Hydrodynamic Diameter nm	Derived count rate kcps	ζ-potential mV	Particle number ×10^8 particles/mL
NPs	0.2 ± 0.01	224 ± 4.8	4437.7 ± 25.6	−14.6 ± 3.4	84.6 ± 0.9

Table 2
Compositions of nanoparticles derived from derived from Porcine Bone Soup.

Bone soup NPs	Carbohydrates	Proteins	Lipids	Dry weight
(μg/mL)	48.44 ± 0.59	86.51 ± 3.24	204.01 ± 11.30	450.8 ± 4.64
%	10.75	19.19	45.26	—

%: percentage of proteins, carbohydrates and lipids content vs. dry weight.

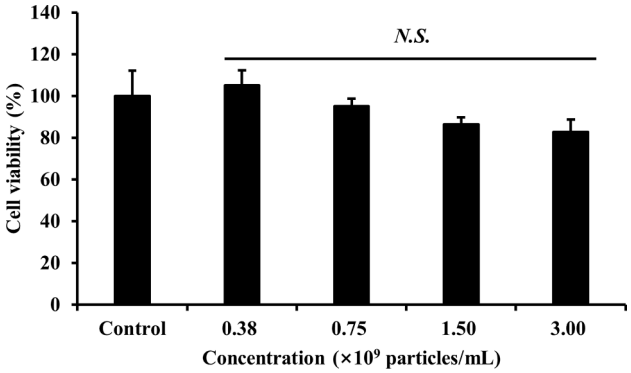

Fig. 2. Cytotoxicity of bone soup NPs on Caco-2 cells *in vitro*. Data were expressed as the mean ± SD ($n = 5$). *N.S.*, no significance, compared to control group by the Student's *t*-test.

At the presence of AAPH, incubation of Caco-2 cells together with bone soup NPs at different concentrations (3.00, 2.25, and 1.5 × 10^9 particles/mL) resulted in elevated CI values. The CI values recovered by the NPs were slightly lower than the normal cells in the first 30 min. However, the CI values of monolayer treated by the NPs at 3.00 × 10^9 particles/mL became significantly higher than normal cells afterwards, suggesting that bone soup NPs could entirely or partially maintained the normal barrier permeability and consolidated the cell–cell attachment on AAPH-treated Caco-2 cell monolayers.

The tight junctions (TJs) and adherent junctions (AJ) related proteins, including ZO-1, F-actin, and E-cadherin were further investigated by immunofluorescence staining. As shown in Fig.5, the immunofluorescence staining revealed a clearly filamentous arrangement of F-actin was shown in the cell substructure, as well as a continuous distribution of ZO-1 and cadherin on the membrane bound of normal cells. In the presence of AAPH (shown in Fig. 5), F-actin's filamentous arrangement was disrupted, while ZO-1 and cadherin were delocalized from the cell membrane and dispersed across the intercellular space. These phenomena concurred well with the previous studies reported by Mauro (Serafini, 2018). It suggested that the integrity of TJs and AJs was disrupted by AAPH-induced oxidative stresses, together with other adverse consequences on epithelial barrier function, TEER value, and FL permeability. The treatment together with bone soup NPs and AAPH (shown in Fig. 5C) resulted in remaining same structures of F-actin, ZO-1 and cadherin compared with non-treated Caco-2 cell monolayers, suggesting the NPs can restore the AAPH-induced damages on TJs and AJs related proteins. Moreover, as shown in Fig. 5D, the treatment with the NPs alone did not influence TJ and AJ-related proteins on the monolayer.

4. Discussion

Since safety concerns arose on the interaction between nanoparticles in food and the intestinal tract, as a part of daily food, the porcin bone soup NPs are also worth paying attention to. Although whether these NPs were digested or structural modified (e.g. forming protein-corona) after gastrointestinal digestion is remaining unkown, to face the worst, if porcine bone soup NPs can keep their pristine nano structures after

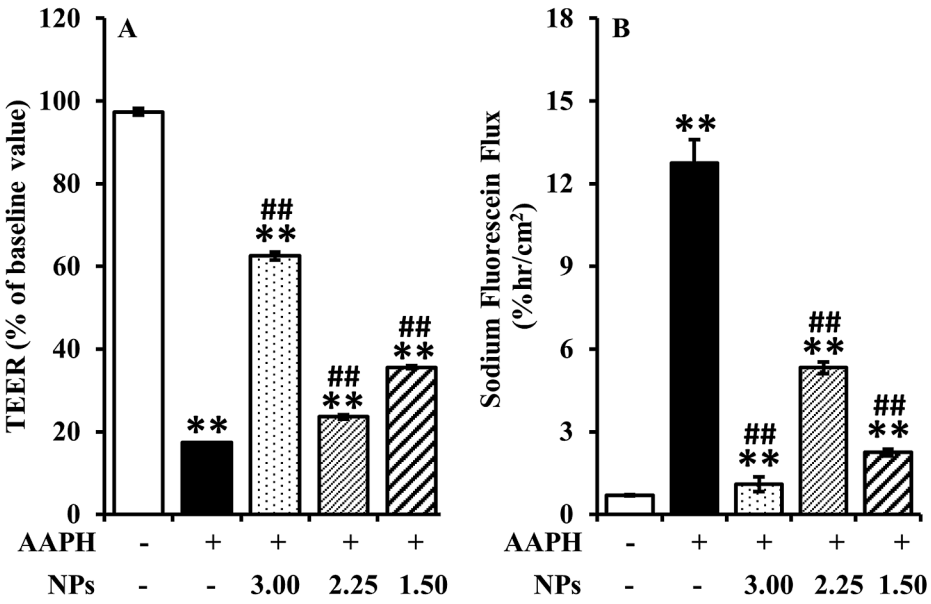

Fig. 3. Effects of NPs isolated from porcine bone soup on Caco-2 cells monolayer induced by AAPH. (a) TEER tendency of NPs isolated from porcine bone soup on AAPH-induced Caco-2 cells at the concentration of 3.00, 2.25 and 1.50 × 10^9 particles/mL after 6 h; (b) Inhibition effects of NPs on the AAPH-induced fluorescein sodium permeability of Caco-2 cells at the concentration of 3.00, 2.25 and 1.50 × 10^9 particles/mL after 6 h. Data were expressed as the mean ± SD ($n = 3$). $^{**}P < 0.01$, $^{*}P < 0.05$, compared to control group; $\#\#P < 0.01$, $\#P < 0.05$, compared to AAPH group by the Student's *t*-test.

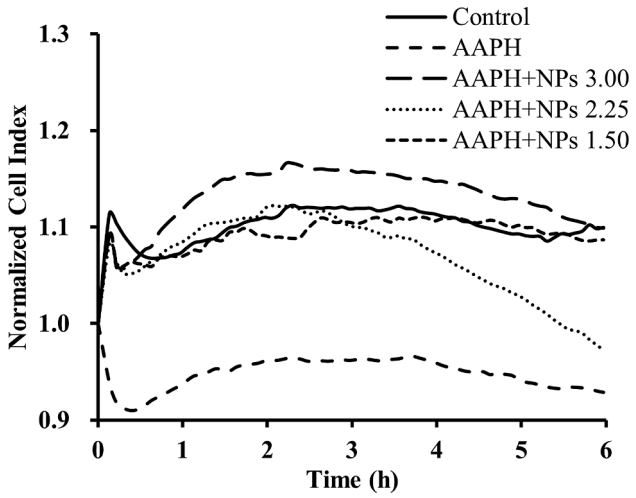

Fig. 4. AAPH-induced epithelial barrier dysfunction and its restoration by bone soup NPs with the xCELLigence system in Caco-2 cells. The panels show representative data averaged from three wells.

gastrointestinal digestion, do they produce any adverse physiological effects on intestinal cells? The bone soup NPs, however, did not exhibit cytotoxicity to Caco-2 cell and other adverse effects on Caco-2 cell monolayer compared with ENMs, which usually injury the barrier's integrity and increased permeability (Brun et al., 2014; García-Rodríguez et al., 2018; Martirosyan et al., 2012; Mortensen et al., 2020; Ruiz et al., 2017; Vita et al., 2019).

Oxidative stress plays a vital role in the initiation and development of intestinal barrier dysfunction (Thomson, Hemphill, & Jeejeebhoy, 1998). In this study, AAPH, which can generate two potent ROS and induce lipid oxidative, has been wide used to trigger oxidative stress in cell model *in vitro* (Serafini, 2018). The spherical NPs isolated from bone soup were demonstrated to protect Caco-2 cell monolayer from AAPH-induced oxidative damage and dysfunction, suggesting the porcine bone soup NPs protected the barrier integrity and permeability of Caco-2 cell monolayer via their antioxidative activity. It has been reported that the reduction of oxidative stress could ameoliate the intestinal barrier dysfunction (Mukojima et al., 2009; Nallathambi, Poulev, Zuk, & Raskin, 2020; Serafini, 2018)

The antioxidant activity of the bone soup NPs may rely on their compositions/bioactive compounds they carry on or their unique physicochemical properties. Our previous study disclosed that the porcine bone soup NPs consisted of proteins, including collagen (Wang et al., 2019). The constitutive collagen of bone soup NPs might contribute to its antioxidant activity and preventing barrier dysfunction induced by AAPH in Caco-2 cell monolayer. Meanwhile, in the present AAPH-induced intestinal barrier injury cell model, oxidative stress caused intestinal barrier dysfunction via disruption of TJs and AJs (Serafini, 2018), and play a vital role in the barrier dysfunction(Rao, 2008). However, the underlying mechanism of bone soup NPs restoring AAPH-induced intestinal barrier dysfunction warranted to investigate.

As a traditional food, bone soup is consumed worldwide not only for its nutrition but also for its efficacy in preventing and treating inflammatory bowel disease (IBD) and immune malfunction (Morell & Daniel, 2014; Siebecker, 2005). IBD usually has tight connections with intestinal barrier dysfunction caused by oxidative stress (Antoni, Nuding, Wehkamp, & Stange, 2014). Besides, dramatic changes in barrier dysfunction, including epithelial TJs structure and paracellular permeability, were also found in ulcerative colitis (UC) (Schulzke et al., 2009) and irritable bowel syndrome (IBS) (Eutamene & Bueno, 2007; Piche et al., 2009). In this study, the nanoparticles isolated from porcine bone soup were observed to significantly alleviate the barrier integrity damage, reduce the FL permeability of Caco-2 cell monolayer induced by oxidative stress, and probably protect the barrier function from oxidative stress injury by retaining TJ (ZO-1), AJ (E-cadherin), and F-actin protein (Fig. 6). Moreover, in our previous studies, the bone soup NPs had also been reported to directly interact with immune cells (oral and peritoneal macrophage) and effectively protected them from oxidative stress-induced cellular malfunction (Ke et al., 2017; Wang et al., 2019). The bone soup NPs effectively attenuate the oxidative stress-induced cellular malfunction.

5. Conclusions

In this study, the effects of bone soup NPs on intestinal barrier function were evaluated on Caco-2 cells monolayers. The results showed that the bone soup-derived NPs protected the barrier integrity and permeability of Caco-2 cell monolayer from oxidative stress. The bone soup NPs significantly alleviated the barrier function damage and restored the AAPH-induced damages on TJs and AJs related proteins. It shows the potential of bone soup NPs as a dietary treatment for intestinal

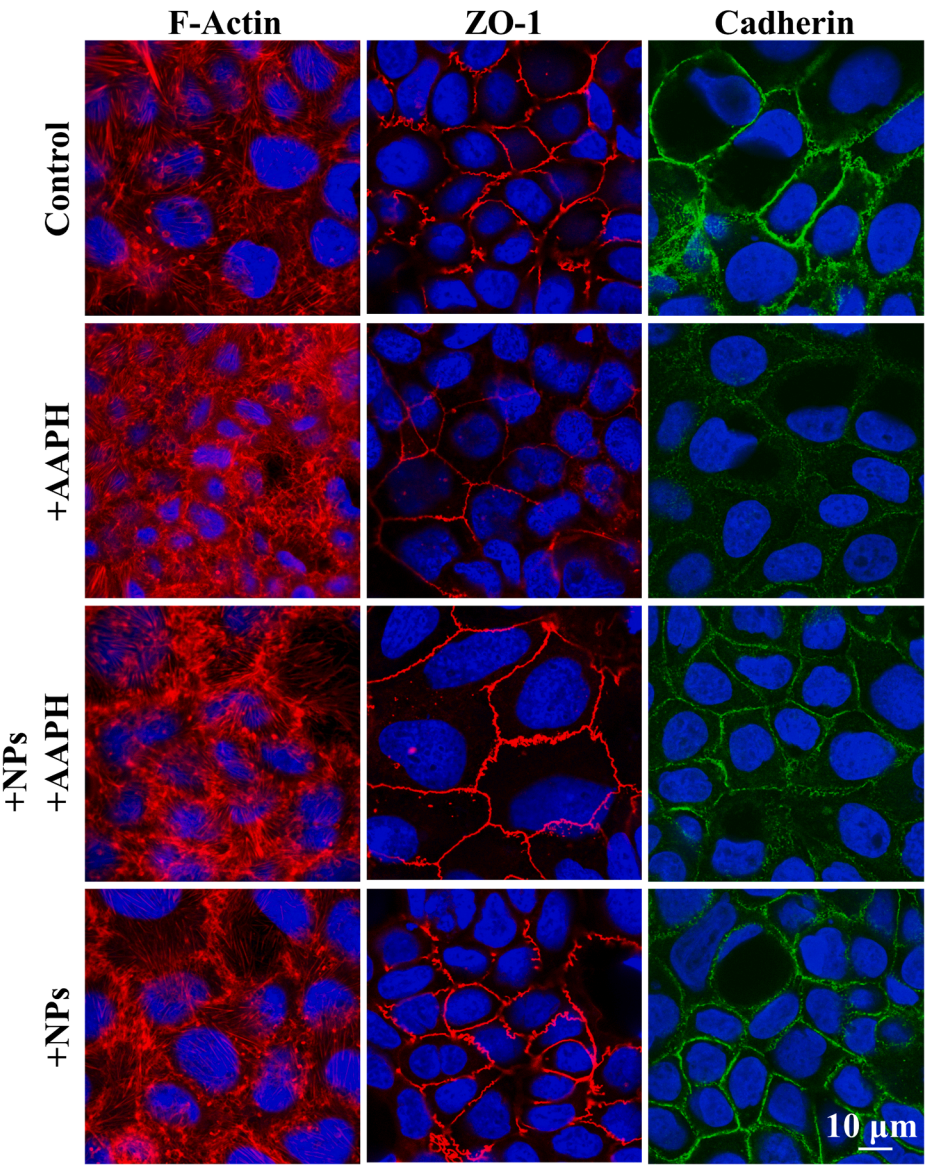

Fig. 5. Effects of NPs isolated from porcine bone soup on the Caco-2 cell monolayer membrane integrity. The group of AAPH, AAPH + NPs, and NPs were added into cell wells and then incubated for 2 h. After immunostaining, Hoechst 33,342 was added into each well. The excitation wavelength/emission wavelength of F-action, ZO-1, Cadherin, and Hoechst 33,342 is 540/564 nm, 590/617 nm, 498/520 nm, and 346/460 nm, respectively. Magnification: ×63. Merged micrograph taken by LCFM software, scale bar = 10 μm.

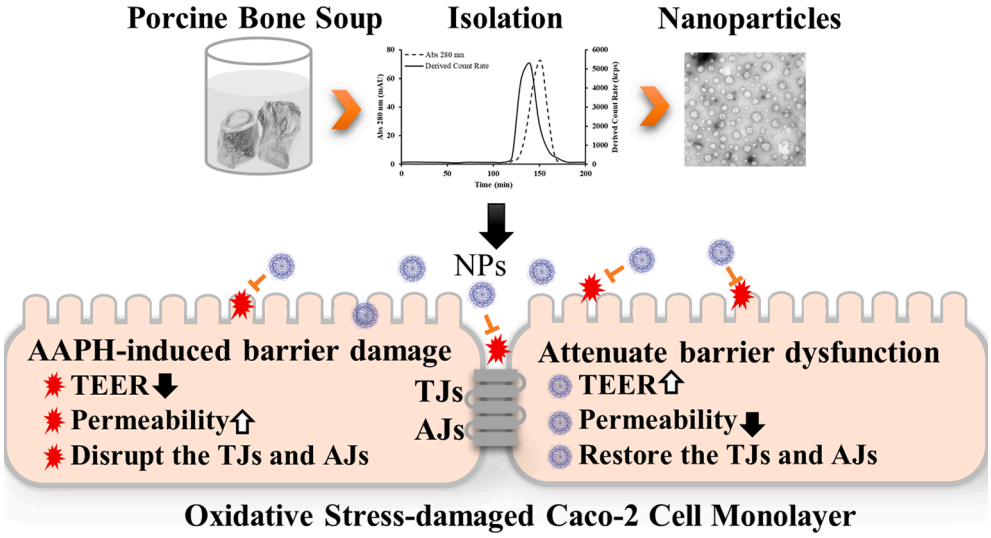

Fig. 6. Schematic diagram of the interaction between porcine bone soup NPs and Caco-2 cells monolayer.

disorders, resonating with the traditional knowledge of bone soup efficacies.

Ethics statement

Our study didn't involve any human subjects and animal experiments.

CRediT authorship contribution statement

Guanzhen Gao: Conceptualization, Data curation, Methodology, Formal analysis, Writing - original draft. **Jianwu Zhou:** Formal analysis, Supervision, Writing - review & editing. **Yongyang Jin:** Data curation, Methodology, Formal analysis. **Huiqin Wang:** Conceptualization, Methodology, Supervision, Investigation, Validation, Funding acquisition, Project administration, Writing - review & editing. **Yanan Ding:** Methodology, Formal analysis, Investigation. **Jingru Zhou:** Methodology, Formal analysis, Investigation. **Lijing Ke:** Formal analysis, Project administration, Writing - review & editing. **Pingfan Rao:** Conceptualization, Writing - review & editing. **Pik Han Chong:** Writing - review & editing. **Qiang Wang:** Writing - review & editing. **Longxin Zhang:** Writing - review & editing.

Declaration of Competing Interest

The authors declare that they have no known competing financial interests or personal relationships that could have appeared to influence the work reported in this paper.

Acknowledgements

This work was supported by the National Key R&D Program of China (2016YFD0400202).

Appendix A. Supplementary data

Supplementary data to this article can be found online at https://doi.org/10.1016/j.jff.2021.104573.

References

Antoni, L., Nuding, S., Wehkamp, J., & Stange, E. F. (2014). Intestinal barrier in inflammatory bowel disease. *World Journal of Gastroenterology, 20*(5), 1165–1179.

Atienza, J. M., Yu, N., Kirstein, S. L., Xi, B., Wang, X., Xu, X., & Abassi, Y. A. (2006). Dynamic and label-freee cell-based assays using the real-time cell electronic sensing system. *Assay and Drug Development Technologies, 4*, 597–607.

Bergin, I. L., & Witzmann, F. A. (2013). Nanoparticle toxicity by the gastrointestinal route: Evidence and knowledge gaps. *Int J Biomed Nanosci Nanotechnol, 3*(1–2), 1–44.

Brun, E., Barreau, F., Veronesi, G., Fayard, B., Sorieul, S., Chanéac, C., … Carrière, M. (2014). Titanium dioxide nanoparticle impact and translocation through ex vivo, in vivo and in vitro gut epithelia. *Particle and Fibre Toxicology, 11*(1), 1–16.

Buzea, C., Pacheco, I. I., & Robbie, K. (2007). Nanomaterials and nanoparticles: Sources and toxicity. *Biointerphases, 2*(4).

Cao, L., Song, X., Song, Y., Bi, J., Cong, S., Yu, C., & Tan, M. (2017). Fluorescent nanoparticles from mature vinegar: Their properties and interaction with dopamine. *Food and Function, 8*, 4744–4751.

Cong, S., Wang, N., Wang, K., Wu, Y., Li, D., Song, Y., … Tan, M. (2019). Fluorescent nanoparticles in the popular pizza: Properties, biodistribution and cytotoxicity. *Food and Function, 10*(5), 2408–2416.

Eutamene, H., & Bueno, L. (2007). Role of probiotics in correcting abnormalities of colonic flora induced by stress. *Gut (Vol., 56*(11), 1495–1497.

Gao, G., Wang, H., Zhou, J., Rao, P., Ke, L., Lin, J. J., … Wang, Q. (2021). Isolation and characterization of bioactive proteoglycan-lipid nanoparticles from freshwater clam (Corbicula fluminea Muller) soup. *Journal of Agricultural and Food Chemistry, 69*(5), 1610–1618.

García-Rodríguez, A., Vila, L., Cortés, C., Hernández, A., & Marcos, R. (2018). Effects of differently shaped TiO2NPs (nanospheres, nanorods and nanowires) on the in vitro model (Caco-2/HT29) of the intestinal barrier. *Particle and Fibre Toxicology, 15*(1), 1–16.

Iacob, S., & Iacob, D. G. (2019). Infectious threats, the intestinal barrier, and its trojan horse: Dysbiosis. *Frontiers in Microbiology, 10*, 1–17.

Jiang, S., Shi, Y., Li, M., Xiong, L., & Sun, Q. (2019). Characterization of Maillard reaction products micro/nano-particles present in fermented soybean sauce and vinegar. *Scientific Reports, 9*(1), 11285.

Ke, L., Wang, H., Gao, G., Rao, P., He, L., & Zhou, J. (2017). Direct interaction of food derived colloidal micro/nano-particles with oral macrophages. *Npj Science of Food, 1*(3), 1–8.

Ke, L., Zhou, J., Lu, W., Gao, G., & Rao, P. (2011). The power of soups : Super-hero or team-workers? *Trends in Food Science & Technology, 22*(9), 492–497.

Kowapradit, J., Opanasopit, P., Ngawhirunpat, T., Apirakaramwong, A., Rojanarata, T., Ruktanonchai, U., & Sajomsang, W. (2010). In vitro permeability enhancement in intestinal epithelial cells (Caco-2) monolayer of water soluble quaternary ammonium chitosan derivatives. *AAPS PharmSciTech, 11*(2), 497–508.

Lefebvre, D. E., Venema, K., Gombau, L., Jr, L. G. V., Raju, J., Bondy, G. S., Bouwmeester, H., Singh, R. P., Amy, J., Collnot, E., Mehta, R., Stone, V., Raju, J., Bondy, G. S., Bouwmeester, H., Singh, R. P., & Clippinger, A. J. (2015). Utility of models of the gastrointestinal tract for assessment of the digestion and absorption of engineered nanomaterials released from food matrices digestion and absorption of engineered nanomaterials released from. Nanotoxicology, 9(4), 523–542.

Li, S., Jiang, C., Wang, H., Cong, S., & Tan, M. (2018). Fluorescent nanoparticles present in Coca-Cola and Pepsi-Cola: Physiochemical properties, cytotoxicity, biodistribution and digestion studies. *Nanotoxicology, 12*(1), 49–62.

Lin, X., Gao, X., Chen, Z., Zhang, Y., Luo, W., Li, X., & Li, B. (2017). Spontaneously assembled nano-aggregates in clear green tea infusions from Camellia ptilophylla and Camellia sinensis. *Journal of Agricultural and Food Chemistry, 65*(18), 3757–3766.

Martirosyan, A., Polet, M., Bazes, A., Sergent, T., & Schneider, Y.-J. (2012). Food nanoparticles and intestinal inflammation: A real risk? In I. Szabo (Ed.), *Inflammatory Bowel Disease*. IntechOpen.

McClements, D. J., & Xiao, H. (2017). Is nano safe in foods? Establishing the factors impacting the gastrointestinal fate and toxicity of organic and inorganic food-grade nanoparticles. *Npj Science of Food, 1*(1), 1–13.

Mizokami, A., Wang, D. G., Tanaka, M., Gao, J., Takeuchi, H., Matsui, T., & Hirata, M. (2016). An extract from pork bones containing osteocalcin improves glucose metabolism in mice by oral administration. *Bioscience, Biotechnology and Biochemistry, 80*, 2176–2183.

Morell, S. F., & Daniel K, T. (2014). Nourishing broth: An old-fashioned remedy for the modern world. *Hachette Book Group Special Markets Department.*

Mortensen, N. P., Moreno Caffaro, M., Patel, P. R., Uddin, M. J., Aravamudhan, S., Sumner, S. J., & Fennell, T. R. (2020). Investigation of twenty metal, metal oxide, and metal sulfide nanoparticles' impact on differentiated Caco-2 monolayer integrity. *NanoImpact, 17*, Article 100212.

Mukojima, K., Mishima, S., Oda, J., Homma, H., Sasaki, H., Ohta, S., & Yukioka, T. (2009). Protective effects of free radical scavenger edaravone against xanthine oxidase-mediated permeability increases in human intestinal epithelial cell monolayer. *Journal of Burn Care & Research, 30*(2), 335–340.

Nallathambi, R., Poulev, A., Zuk, J. B., & Raskin, I. (2020). Proanthocyanidin-rich grape seed extract reduces inflammation and oxidative stress and restores tight junction barrier function in caco-2 colon cells. *Nutrients, 12*(6), 1623.

Peng, L., He, Z., Chen, W., Holzman, I. R., & Lin, J. (2007). Effects of butyrate on intestinal barrier function in a caco-2 cell monolayer model of intestinal barrier. *Pediatric Research, 61*(1), 37–41.

Piche, T., Barbara, G., Aubert, P., Des Varannes, S. B., Dainese, R., Nano, J. L., … Neunlist, M. (2009). Impaired intestinal barrier integrity in the colon of patients with irritable bowel syndrome: Involvement of soluble mediators. *Gut, 58*(2), 196–201.

Rao, R. (2008). Oxidative stress-induced disruption of epithelial and endothelial tight junctions. *Frontiers in Bioscience, 13*(9), 7210–7226.

Ruiz, P. A., Morón, B., Becker, H. M., Lang, S., Atrott, K., Spalinger, M. R., … Rogler, G. (2017). Titanium dioxide nanoparticles exacerbate DSS-induced colitis: Role of the NLRP3 inflammasome. *Gut, 66*(7), 1216–1224.

Salvo-Romero, E., Alonso-Cotoner, C., Pardo-Camacho, C., Casado-Bedmar, M., & Vicario, M. (2015). The intestinal barrier function and its involvement in digestive disease. *Revista Espanola de Enfermedades Digestivas, 107*(11), 686–696.

Schulzke, J. D., Ploeger, S., Amasheh, M., Fromm, A., Zeissig, S., Troeger, H., … Fromm, M. (2009). Epithelial tight junctions in intestinal inflammation. *Annals of the New York Academy of Sciences, 1165*, 294–300.

Serafini, M. (2018). Redox role of lactobacillus casei shirota against the cellular induced oxidative and inflammatory stress in enterocytes-like epithelial cells. *Frontiers in Immunology, 9*(1131), 1–12.

Siebecker, A. (2005). Traditional bone broth in modern health and disease. *Townsend Letter, 259*(260), 74–81.

Sinnecker, H., Krause, T., Koelling, S., Lautenschläger, I., & Frey, A. (2014). The gut wall provides an effective barrier against nanoparticle uptake. *Beilstein Journal of Nanotechnology, 5*(1), 2092–2101.

Sun, M., Fu, H., Cheng, H., Cao, Q., Zhao, Y., Mou, X., … Ke, Y. (2012). A dynamic real-time method for monitoring epithelial barrier function in vitro. *Analytical Biochemistry, 425*(2), 96–103.

Thomson, A., Hemphill, D., & Jeejeebhoy, K. (1998). Oxidative stress and antioxidants in intestinal disease. *Dig Dis., 16*(3), 152–158.

Vila, L., García-Rodríguez, A., Cortés, C., Marcos, R., & Hernández, A. (2018). Assessing the effects of silver nanoparticles on monolayers of differentiated Caco-2 cells, as a model of intestinal barrier. *Food and Chemical Toxicology, 116*, 1–10.

Vita, A. A., Royse, E. A., & Pullen, N. A. (2019). Nanoparticles and danger signals: Oral delivery vehicles as potential disruptors of intestinal barrier homeostasis. *Journal of Leukocyte Biology, 106*(1), 95–103.

Wang, H., Gao, G., Ke, L., Zhou, J., Rao, P., Jin, Y., … Wang, Q. (2019). Isolation of colloidal particles from porcine bone soup and their interaction with murine peritoneal macrophage. *Journal of Functional Foods, 54*, 403–411.
Wang, N., Wang, G., Hao, J. X., Ma, J. J., Wang, Y., Jiang, X. Y., & Jiang, H. Q. (2012). Curcumin ameliorates hydrogen peroxide-induced epithelial barrier disruption by upregulating heme oxygenase-1 expression in human intestinal epithelial cells. *Digestive Diseases and Sciences, 57*(7), 1792–1801.
Zhou, J., Gao, G., Chu, Q., Wang, H., Rao, P., & Ke, L. (2014). Chromatographic isolation of nanoparticles from Ma-Xing-Shi-Gan-Tang decoction and their characterization. *Journal of Ethnopharmacology, 151*(3), 1116–1123.